Solid Freeform Fabrication 2024: Proceedings of the 35th Annual International
Solid Freeform Fabrication Symposium – An Additive Manufacturing Conference
Reviewed Paper

Design and Fabrication of a Multi-Directional Aerial 3D Printer

Jacob Lasso-Garifalis[1], Alex Pan[1], Elijah Olowokere[1], Otgondulam Boldbaatar[1], Alaina Villanueva[1], Lucas Vergara[1], Suyog Ghungrad[1], Jonathan Komperda[1], Azadeh Haghighi[1]

[1]Department of Mechanical and Industrial Engineering, University of Illinois Chicago, Chicago, USA.

Abstract

Aerial 3D printing is an emerging technology that aims to overcome several limitations of traditional additive manufacturing platforms, specifically constraints associated with print size and accessibility (e.g., at high altitudes). An aerial 3D printer integrates an Unmanned Aerial Vehicle (UAV) with the additive manufacturing technology for targeted deposition of material, enabling automated manufacturing, maintenance, and repair at hard-to-access locations such as high-rise buildings and bridges. However, the existing state-of-the-art aerial 3D printers cannot accommodate multi-directional material deposition, e.g., for conformal printing over complex or angular surfaces. To address this gap, this work presents the design and fabrication of a first-ever multi-directional aerial 3D printer. Various design alternatives for the deposition head were considered and analyzed with respect to weight, functionality, and rigidity metrics. Finally, successful multi-directional material deposition using an expanding foam has been demonstrated with the fabricated prototype.

1. Introduction

In the current state of additive manufacturing (AM), the most common machine is a traditional gantry-based 3D printer [1]. While 3D printing has transformed modern manufacturing, it is limited to a fixed frame that requires the user to either print a product that is smaller than the volume of the printer itself or divide the product into multiple parts and attach them afterward [2,3]. Recent research in novel AM systems aims to transcend this build volume limitation. This led to the development of mobile robotic arms or drones to perform additive manufacturing, having no constraints on the build envelope and scale of the part [4–8]. In particular, drone printing is beneficial in minimizing safety risks and expenses in situations involving high, hostile, or unreachable terrains that pose dangers to humans or are difficult to navigate with ground-based techniques. An example use-case is the façade/structural maintenance of high-rise buildings. For many current-standing high-rise buildings, there are a multitude of factors that contribute to a high cost of maintenance, many of which stem from design deficiencies. One of the five main factors is the inaccessibility of maintenance work, stemming from a lack of initial consideration for equipment such as ladders, gondolas, lifts, and scaffolding [9]. Inhibitors such as these exacerbate the already high maintenance cost due to the additional accommodation, time, restriction of periodic maintenance, and safety concerns for residents and workers.

Few 3D printing drones have been built and demonstrated the capability to print an object on a surface, as shown in Figure 1, but these early editions have a glaring limitation [6–8]. Currently, AM drones are limited to vertical extrusion, only allowing the construction of vertical structures such as pillars or bases. The lack of controlled angular deposition of material for drone-based additive manufacturing means that the technology cannot be applied to use cases on pre-existing structures or steeper surfaces with unique geometries. Additionally, vertical or planar printing

causes a staircase effect [10], and printing along curved surfaces can solve the problem [11], as shown in Figure 2. Hence, the primary goal of this work is to design and fabricate a drone with angular printing capabilities.

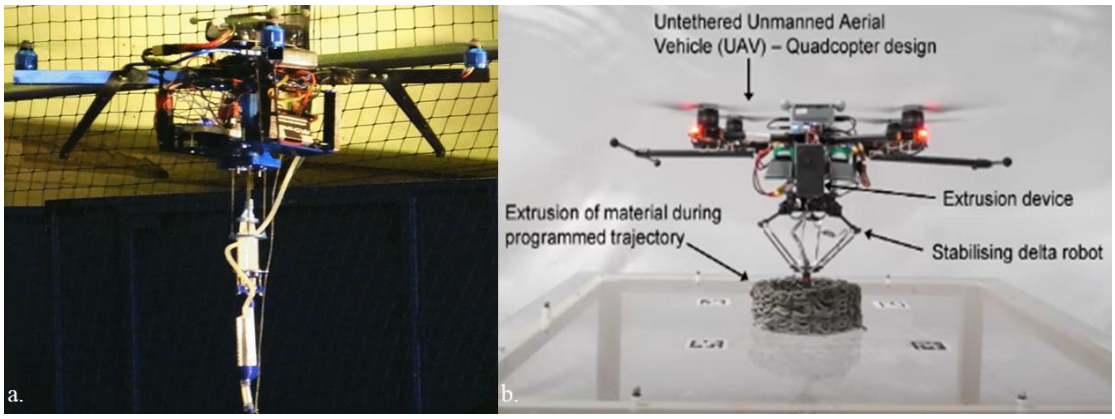

Figure 1: Different aerial additive manufacturing drones a. drone for fused deposition modeling technique [6]. b. drone with delta robot mechanism [7]

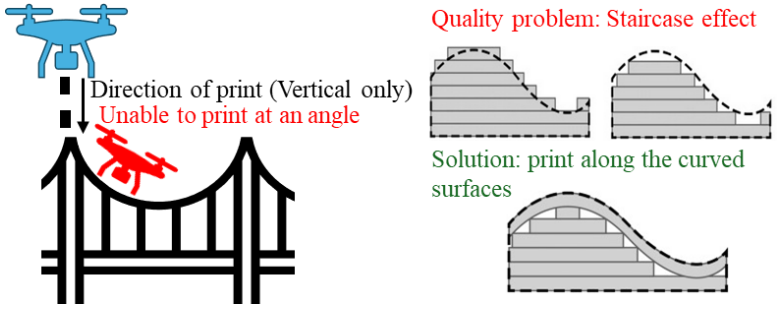

Figure 2: Limitations of current drone-based additive manufacturing

In this work, three extruder mechanisms are designed for angular deposition, and well-defined metrics for selecting and evaluating them have been considered. The most important factor is the force impact on mechanisms while printing and flying, which has been evaluated in the Ansys simulation. There are other design challenges, such as the drone's payload capacity, printing process, and material compatibility for the drone. Furthermore, design and fabrication iterations are discussed before making the drone capable of angular deposition. This work demonstrates a fully functional and autonomous drone with controlled angular deposition of construction material.

2. Methodology

2.1 Design metrics

There are eight design metrics for defining the success of the drone for angular deposition. Their definition and measurement steps are presented in Table 1. The most important metrics are accurate rotational extruder head, which can cover positions within a 180-degree range, and the user's safety should not be compromised. Other criteria have been considered, such as the total cost of the project and the availability of the materials/components, but they are fixed and previously known, so they are excluded from Table 1. The least expensive drone in the market

meeting needs, i.e., PX4 Development Kit - X500 v2 paired with a 5000mAh battery, was chosen. The drone can carry a payload of 1.5kg, but due to the battery weighing 500g, the total allowed payload mass is about 1kg. Furthermore, the drone comes with landing gear (legs that extend), assuring a safe landing even with the arm, battery, and can of foam mounted under the drone.

Table 1: List of all design metrics

Metrics	Definition	Measurement
Accurate Rotational Extruder Head	Extruder head should be able to cover positions within a 180-degree range	Difference in distance between projected coordinates vs actual
Extruder: Reliability	Material exits the extruder	Consistent line widths and heights at flow rates
Safety	Operator should be safe while using the drone	Recording any injuries during testing. Toxicity of materials used, exposure to propellors, battery safety, range and lethality of shrapnel upon failure
Material Efficacy and Durability	Material usefulness for repairs	Density/ payload weight, shelf life; Final hardness, brittleness, lifespan, reactivity to environment, adhesion to repair surfaces
Range/ Usable duration	Time for drone to remain air-born and perform printing tasks	Duration of the flight of the drone at full payload capacity with constant extrusion until failure
Overall Durability (Drone and Extruder)	Lifespan and durability of all components	Battery life, mechanical wear of components, overall impact resistance, overall expected lifespan.
Ease of Development	Difficulty to use and to modify for future developments	Number of stages/ components need to be removed or added to integrate ideas for future research ideas
Ease of Use	Easiness in reading and accessing the user interfaces and manuals	Number of manual pages to read by user to understand with accessibility options

2.2 Extruder mechanism

Three different mechanism designs were evaluated. The first design is a long, rigid arm set at an angle connected to the drone with a pivoting point at the nozzle, as shown in Figure 3a. The second one uses a long rotating arm whose pivot point is near the drone body, as shown in Figure 3b. The third design uses a gear train to drive a pivoting arm with a fixed nozzle and a counterweight to provide stability, as shown in Figure 3c. The decision matrix is based on the following metrics: range of motion, number of linkages, number of joints, manufacturability, moment at extreme angles, and torque required for motion. To quantify the efficacy of each design, each one was simulated with the applied propulsion force from the deposition of the additive manufacturing material. Due to the intent of the arm being mounted on a drone, the single most important criterion of those evaluated is the weight due to the hard constraint of the drone's payload capacity. The Ansys simulation utilizes a static load of 5N vertically onto the arms to detail the thrust applied by the foam during the extrusion process. The first design was decided as the most feasible due to the clearance from the drone, as well as an acceptable weight, moment, and reaction force. The second design did not have enough clearance and the third design was the heaviest. Based on the ANSYS results, the first arm design offered the best results due to having the lowest weight of the three in addition to high rigidity.

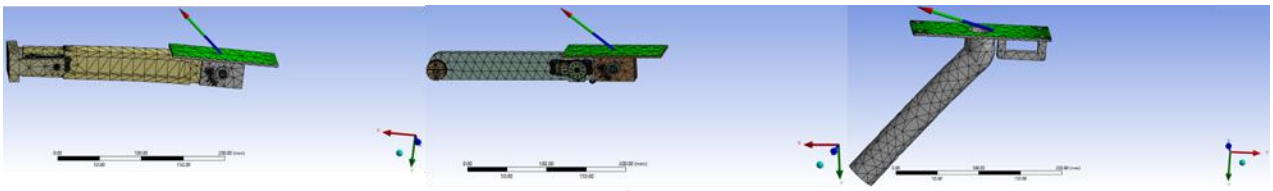

a. b. c.

Figure 3: Three different extruder mechanisms for drone-based AM from Ansys simulation results with a resultant force reaction due to static load of 5N

2.3 Extruder mechanism material

Different materials, from ABS plastic to aluminum metal, were considered. First, different types of engineering plastics (i.e., UHMW polyethylene plastic, acetal plastic, nylon plastic, cast nylon plastic, HDPE polyethylene plastic, PVC plastic, ABS plastic, polycarbonate plastic, polypropylene plastic, PTFE (Teflon) plastic, and cast acrylic plastic) and aluminum (i.e., aluminum 6061, aluminum 6063, aluminum 6013, aluminum 2024, aluminum 7075, and aluminum 2011) were compared for different metrics such as tensile strength, cost on McMaster-Carr per unit volume, coefficient of thermal expansion, flexural modulus, minimum hardness, density, and impact strength per unit density. The scoring system used physical properties and applied linear scales between the maximum and minimum measurements of the different metrics. After combining all the scores, the top three were UHMW Polyethylene, ABS Plastic, and Cast Acrylic among the engineering plastic and Aluminum 6063, Aluminum 7075, and Aluminum 6061 among the aluminum group.

The next step was to compare the best three from the aluminum and plastic groups and four metrics: Yield Strength/Tensile strength, cost per unit volume, density, and strength per unit density. When the same weight values were applied, the plastics neared 100 points while the aluminum was all around 60 to 70 points, as shown in Table 2. Cast acrylic ranked the highest among all materials with a score of 103, and as a result, it was selected as the desired prototyping material for assembly.

2.4 Extrusion material

After considering thez mechanism type and construction material, the next important design parameter was the deposition material. Two categories of materials, foam [12] and thermoplastics, were considered. However, after further consideration, thermoplastics were disqualified due to the weight and power constraints as they would require a heating element. The three selected foams were rigid polyurethane foam, expanded polystyrene foam, and foam concrete. They were evaluated based on compressive strength, tensile strength, and density. Based on these criteria, the design matrix determines foam concrete is the best material for use, as shown in Table 3. Foam concrete offered the best result among the foam materials, but due to the lack of commercial availability, the polyurethane foam was used for the initial prototyping purposes. In future works, foam concrete can be reconsidered and potentially fabricated for more specific applications.

Table 2: Design and selection matrix of mechanism materials: comparing plastic and aluminum

	Yield Strength (psi)			**Cost per unit volume on McMaster Carr (Dollars/cu.in)**			**Density (lb/cu.in)**			**Yield Strength per unit density (ft-sqr.in.)**			
Material	Measured Value	Raw Score	Weighted Score	Measured Value	Raw Score	Weighted Score	Measured Value	Raw Score	Weighted Score	Measured Value	Raw Score	Weighted Score	Final Score
UHMW Polyethylene	4350	1.0	1.0	$ 0.63	9.5	47.6	0.034	9.9	39.5	127941.2	1.8	9.2	97
ABS Plastic	4200	1.0	1.0	$ 0.58	9.8	48.8	0.033	10.0	40.0	127272.7	1.8	9.1	99
Cast Acrylic Plastic	10000	1.8	1.8	$ 0.53	10.0	50.0	0.043	8.7	34.7	232558.1	3.3	16.3	103
Aluminum 6013 Metal	50000	7.0	7.0	$ 1.72	4.2	20.9	0.098	1.4	5.6	510204.1	7.1	35.4	69
Aluminum 7075 Metal	73000	10.0	10.0	$ 2.37	1.0	5.0	0.101	1.0	4.0	722772.3	10.0	50.0	69
Aluminum 6061 Metal	6600	1.3	1.3	$ 1.01	7.7	38.3	0.098	1.4	5.6	67346.9	1.0	5.0	50
Max Value	73000	10.0	10.0	$ 2.37	1.0	5.0	0.101	1.0	4.0	722772.3	10.0	50.0	69
Min Value	4200	1.0	1.0	$ 0.53	10.0	50.0	0.033	10.0	40.0	67346.9	1.0	5.0	96
Score Weighting Value	1			5			4			5			15

Table 3: Design and selection matrix of extruding foam material

	Compressive Strength (Mpa)			**Tensile Strength (Mpa)**			**Density (kg/m^3)**			
Material	Measured Value	Raw Score	Weight Score	Measured Value	Raw Score	Weight Score	Measured Value	Raw Score	Weight Score	Final Score
Rigid polyurethane foam	0.16	10	50	0.41	10.23	51.125	48	10	30	131.13
Expanded Polystyrene	0.44	25.75	128.75	0.6	14.5	72.5	48.05	10.01	30.03	231.28
Foam Concrete	1	57.25	286.25	0.4	10	50	400	76	228	564.25
Max Value	1	57.25	286.25	0.6	14.5	72.5	400	76	228	586.75
Min Value	0.16	10	50	0.4	10	50	48	10	30	130
Score Weighting Value	5			5			3			13

2.5 Electronics design and integration

The next step was to design a subsystem to operate and control it. It was built with an arduino nano microcontroller, two potentiometers, and two positional servos as shown in Figure 4. For this system, the precise control of the motors is imperative, and it was handled by a custom program. The code can be broken down into two modes: Manual and Automatic, both of which are chosen and operated in the serial monitor. To switch modes, simply reset the arduino and it will start again. Manual mode allows for a user to control each servo motor by turning the potentiometers. This mode is great for use in a demonstration and for testing proper motion, as the user can move the servos slower in manual mode than in automatic mode.

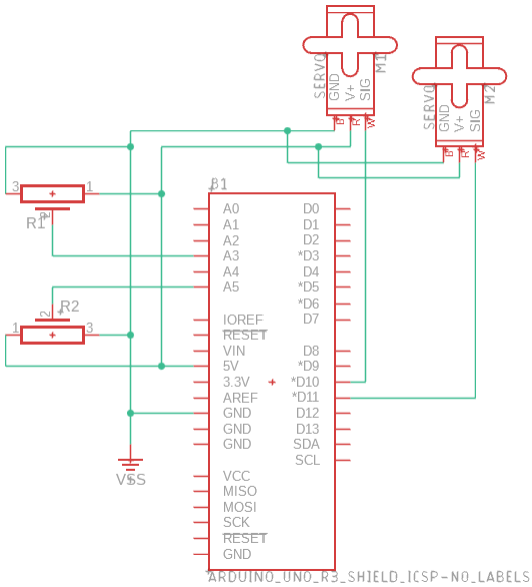

Figure 4: Circuit diagram for electronics

Automatic mode controls the position of each motor based on user inputs. The code is qualitatively described in Figure 5. Once this mode is chosen, the device asks if each motor should be activated. If either one is active, the user will then need to input the extrusion time, or dwell period. After that, the program will ask what angle between 0 and 90 degrees the nozzle should be pointed at if the swivel motor is active. At which point, the nozzle will move to the angle. Then, the program will prompt what power the extrusion should be on a scale of 0 to 100. The program will map that value to an angle position and move there. At this point, foam is flowing through the mechanism, so it will maintain both motor positions for the specified dwell period. After completing the dwell period, both motors will return to initial positions and the loop will start again with asking which motors should be active. Like Manual mode, Automatic mode can be used for a demo. This mode was also designed to be user-friendly for carrying out experiments, since users can specify all the independent variables for testing.

In addition to the two operating modes, the code has internal checks as well as adjustments for hardware. The program has an error message for users who select an invalid mode. It also defines all constant values for operation at the beginning of the code. This is useful for adding an angle offset for servos, defining the delay period between servo commands, maximum values from potentiometers, and total travel angle of the pump servo. This is a pivotal development of this project as without it, there would be no reliable way to control the final result.

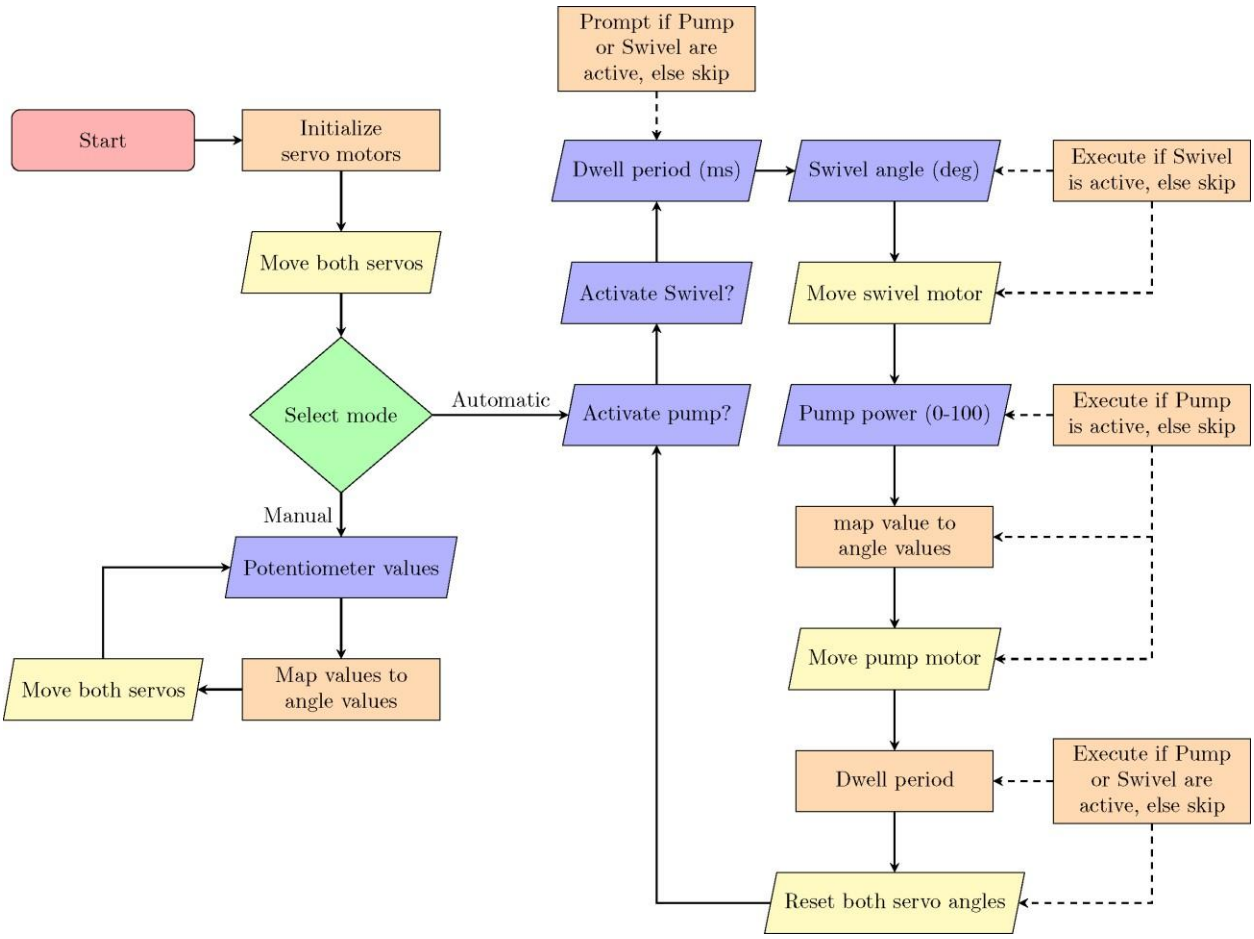

Figure 5: Logic Diagram for Arduino code: orange: internal code process, purple: serial monitor input, yellow: output

3. Fabrication and design improvements

Using laser-cut acrylic sheets, several prototyping iterations were built to physically evaluate each design's efficacy and make necessary improvements. The first design iteration was the original model as shown in Figure 6a**.** The arm is a simple beam with two wheels to translate the rotation of the motor near the base to the end for angling the extruder head. The second iteration of the arm came after completing a topology study of the arm. Using the built-in SolidWorks tools and verifying the structural integrity of the arm with ANSYS, the second arm model was completed with a roughly 48% reduction in weight. Additionally, several holes were added at the base of the arm to physically test out several angles to see the effect each angle had on the applied moment by the arm on the drone. The third iteration extended the baseplate to mount a second motor and spray gun for the expanding foam. The spray gun as shown in Figure 6c is a modified version of Great Stuff's Pro Dispensing Gun, cut down to reduce weight and length. In practice, foam will be extruded through a tube with a nozzle connected at the end. Due to the inclusion of the spray gun, a second motor was needed to trigger the spray. The belt and gear system was tested with the timing belt temporarily secured around the gears and was able to rotate the nozzle tip for angular 3D printing. Additionally, the arm base is chamfered to allow the arm to move through the different angles without obstruction. The fourth iteration addressed a previous design flaw where the foam canister needed to be inverted for the foam to flow properly. A new base was designed that allowed the canister to be slotted in and fixed at 3 different distances. Additionally, a slot was designed at

the end of the arm so that the belt tension could be adjusted. The third major change was a motor mount that connects to the back of the modified spray gun. The function of the motor mount is to control a simple cam and follower assembly for the actuation of the spray foam. The prototype for this iteration had the first full permanent assembly of the belt and gear system. The timing belt was cut to loop around the shortest distance of the slot so the bolt could be moved down the slot to tension the belt. It is worth mentioning that longer legs were machined to allow the necessary clearance for the canister due to its length, these were later replaced with carbon fiber tubes.

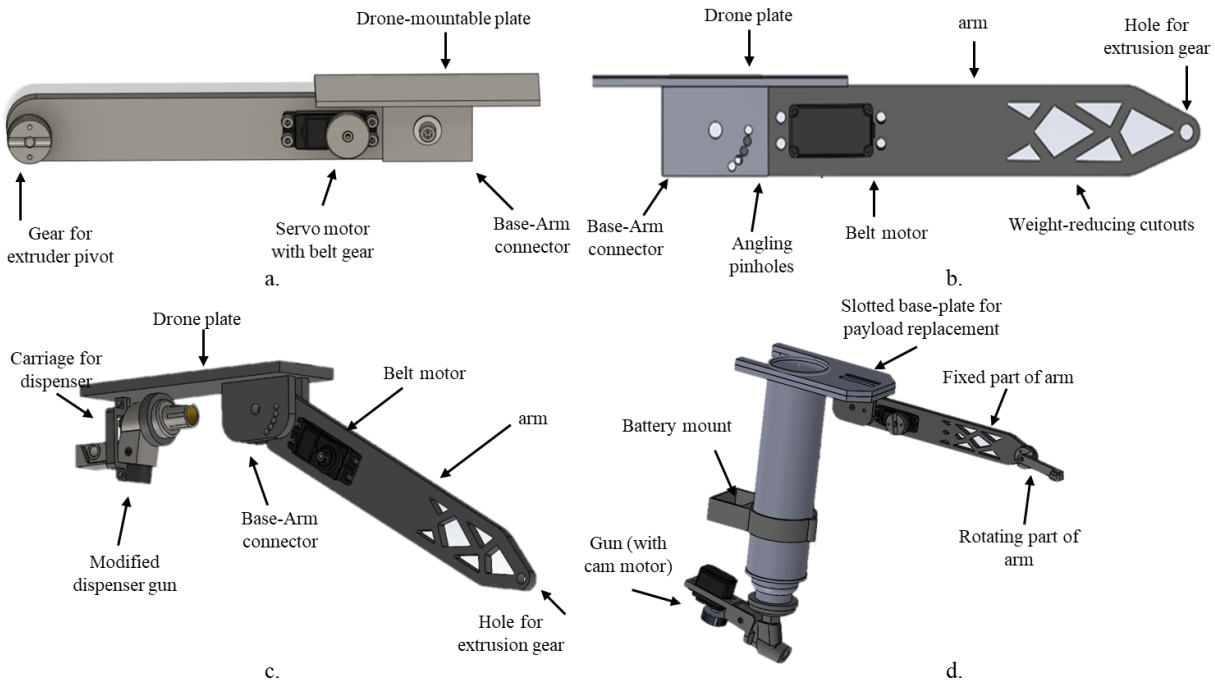

Figure 6: First iteration (original design). b. Second iteration. c. Third iteration. d. Fourth iteration of design and fabrication improvements

4. Aerial 3D printing

The total allowed payload mass is about 1kg, which exceeds the total mass of our fabricated components and attachments, including the arm, can of foam, and multiple motors. Figure 7 shows the full assembly of the arm and payload while mounted to the drone. As seen in Figure 7, the prototype functions as follows: The foam gun is screwed to the adapter at the top of the polyurethane canister. A servo-controlled cam and follower pin open and close the nozzle, actuating the flow. When open, the pressure in the canister sends the foam through vinyl tubing which is fixed to the belt-driven gear controlled by a second servo motor. To test the prototype, the motors and Arduino were connected and ran with the code with the foam canister loaded to confirm that all systems worked together. The initial full test showed that all systems could successfully work together, controlling the flow of the foam and the angle of deposition. Figure 8 shows the success of controlled angular deposition when drone is on ground. Additionally, the foam was able to be extruded onto a vertical surface and multiple other angles. Further testing with the final iteration showed that the spring used to keep the follower closed had to overcome greater forces after the initial use. This could be due to some foam remaining on some components even after cleaning. This was solved by using a stronger spring which consequently caused the 3d-

printed cam and motor holder to bend. The cam and a reinforcing plate were then made in aluminum to prevent bending.

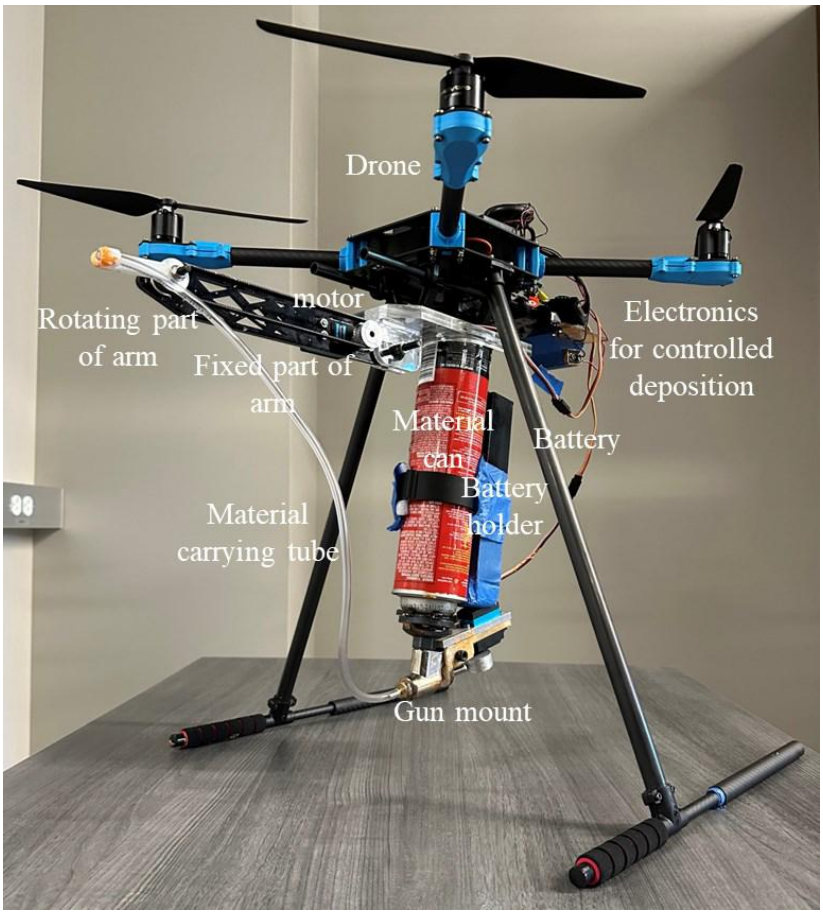

Figure 7: Fourth iteration of drone arm design whilst mounted to the drone

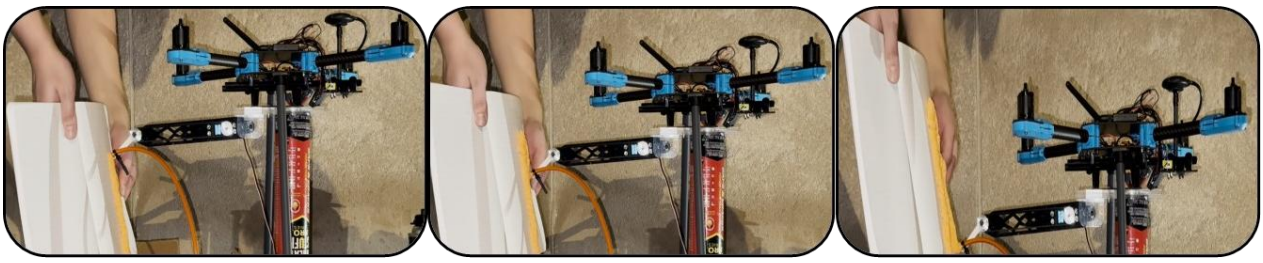

a. Track 1 b. Starting track 2 c. Completion of track 2

Figure 8: Successful demonstration of controlled angular deposition at 45-degree angle with drone on ground

The next phase was to 3D print when flying the drone. The systems used to handle flight path planning and autopilot are QGroundControl (QGC), an open-source ground control station, and PX4, an open-source flight control software. The drone has a PX4 flight controller pre-installed, and QGC is installed on the user system. Figure 9 captures the user interface during flight missions, which is a satellite image of the flight space with an active monitor for the drone's position. Using

QGC, a flight mission can be planned and then uploaded to the drone via USB. The drone is equipped with a GPS to report its position to mission control and will correct course if needed. The drone and the laptop communicate via the telemetry radio system, where the first radio is connected to the onboard controller and the second is connected to the navigating laptop via USB. Factors that can be set include the takeoff position, takeoff altitude, travel path, travel speed, travel altitude, and landing position. A geofence was also set to prevent the drone from drifting too far, as shown in Figure 9.

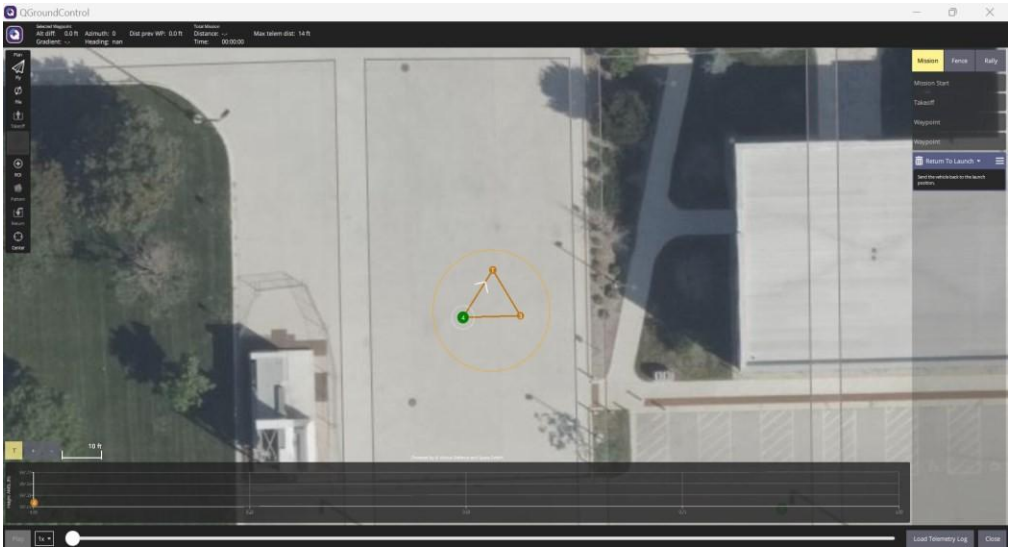

Figure 9: QGC demonstration of a three-position flight path (triangle) encapsulated by a circular geofence to limit drone position in case of miscommunication and/or external events such as high winds.

After integrating the drone flight path and 3D printing location and path, the drone can autonomously fly to the target location and perform 3D printing. An experiment with indoor settings and manual control of drone to have a stable fly at a certain height from ground and then depositing the foam on target surface was performed. First demonstration was on horizontal print surface with 0 line spacing for two tracks and second demonstration was on 30-degree print surface with 10 cm line spacing for two tracks. Figure 10 demonstrates a drone depositing material at 60- and 30-degree angles on the horizontal surface and 30- and 0- degree angles on the 30^{o} print surface for 20 seconds. The first step is drone flying and being stable within first 10 seconds and then material starts flowing into the extruder tube from 9th second. The arm turns first to 60 degrees and material starts depositing the first track for 5 seconds and then for the second track, the arm turns to 30 degrees. After 20 seconds, the can is closed and for the next 10 seconds drone holds the position and slowly lands. The final print (Figure 10d) has huge material deposits at the end point due to the remaining material gushing out of the tube even after closing the foam. The propeller drag force caused the material coming out of tube to float in air for some time and even flow away if the stand-off height between the extruder and the print surface was high on horizontal print surface. Similar steps were followed for printing on 30-degree print surface as shown in Figure 10e-h. In 30-degree print surface, the change of angle caused the width of print to change and the drone moving quickly caused a discontinuity in the entire path. This leads to future research in numerical simulation models for accounting wind drag from propellers on to the material extruding and improving the design mechanism.

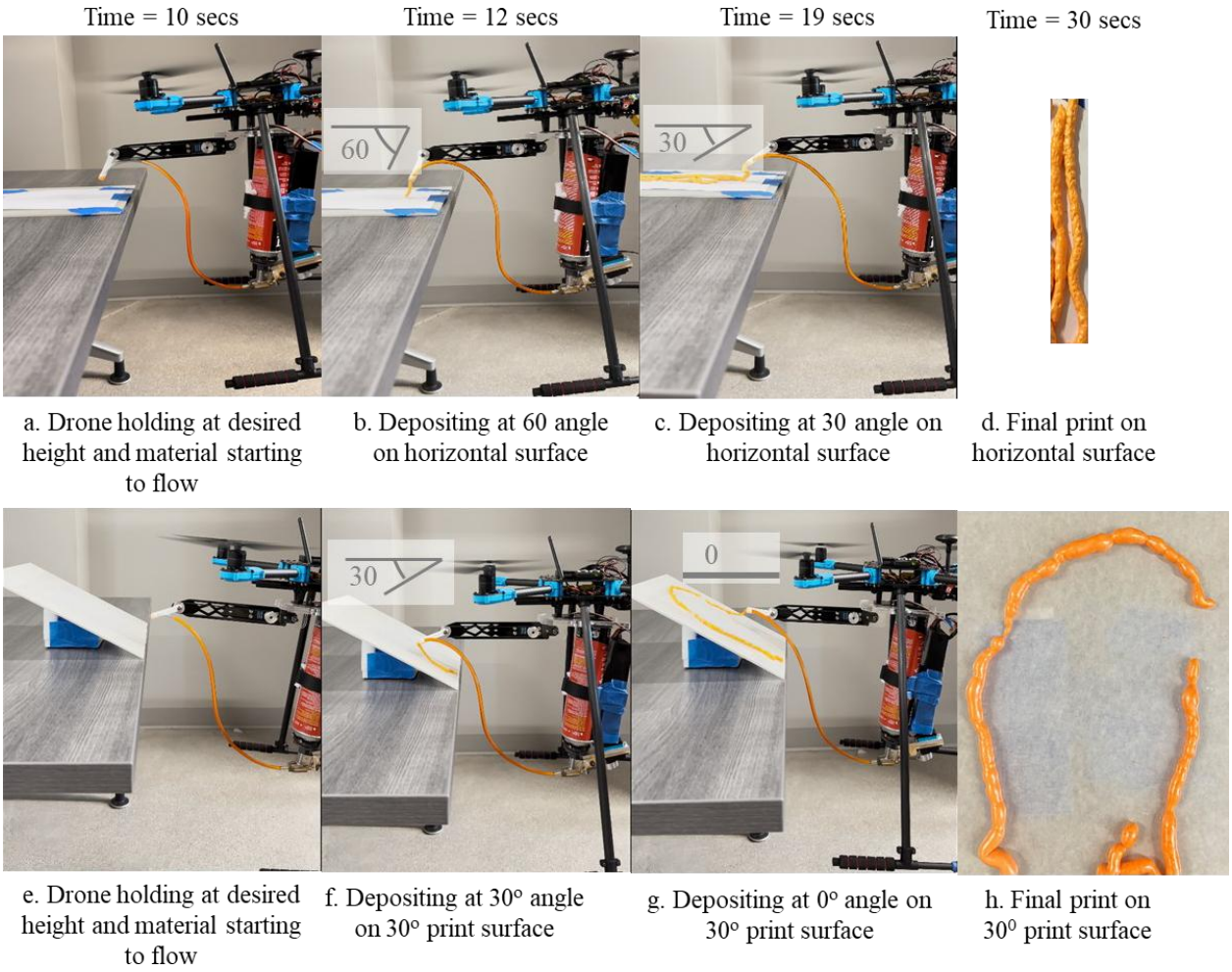

Figure 10: Successful demonstration of drone depositing at 60- and 30- degree angles on a horizontal surface

5. Conclusion and future work

Aerial 3D printing is an emerging technology that aims to overcome several limitations of traditional additive manufacturing platforms, specifically constraints associated with print size and accessibility (e.g., at high altitudes). An aerial 3D printer integrates an Unmanned Aerial Vehicle (UAV) with the AM technology for targeted deposition of material, enabling automated manufacturing, maintenance, and repair at hard-to-access locations such as high-rise buildings and bridges. This work addresses the existing gap with aerial 3D printers that is they are unable to have multi-directional material deposition, e.g., for conformal printing over complex or angular surfaces by designing and fabricating a first-ever multi-directional aerial 3D printer. Multiple design metrics for success of the demonstration were considered from functionality, safety to ease of use. Three design alternatives for the extruder were considered and analyzed with respect to weight, functionality, and rigidity metrics. Ansys simulations were performed to evaluate its strength capabilities. To decide extruder and extrusion material, design matrices were utilized. Four fabrication design improvements were made before finalizing the fully function drone for controlled deposition. A successful multi-directional material deposition using an expanding foam has been demonstrated with the fabricated prototype.

There are many exciting future research directions exist. Improving the extruder mechanism to account for wind forces from propeller and increasing the flow rates accordingly. The accuracy and quality of depositing will be analyzed and studied. Impact of different factors such as angle of print, extrusion pressure, extruder stand-off height and direction of print on the geometrical dimensions and mechanical properties will be studied. Feedback control for the drone in real-time due to environmental changes and back pressure from the deposition of foam and payload change while printing will be incorporated. It could be preventing catastrophic failure in the case of automated control by a drone-locating positional sensor and depth sensor. Such sensors are crucial on all 6 sides of the drone to prevent the automated controller from crashing the drone into the surface. With the close-quarters nature of the drone's deployment to different structures, there will be cases of which the drone has a small space to work in. While the control system could instruct the drone to adjust based on the deposition, there is a current lack of sensors to indicate whether the drone is at risk of making direct contact with a surface. It would be crucial to introduce those simpler positional sensors to allow the companion computer to contextualize the drone to its working space and develop strict limitations to prevent such failures.

References

[1] Khosravani MR, Haghighi A. Large-Scale Automated Additive Construction: Overview, Robotic Solutions, Sustainability, and Future Prospect. Sustain 2022;14. https://doi.org/10.3390/su14159782.

[2] Poudel L, Sha Z, Zhou W. Mechanical strength of chunk-based printed parts for cooperative 3D printing. Procedia Manuf 2018;26:962–72. https://doi.org/10.1016/j.promfg.2018.07.123.

[3] Ghungrad S, Haghighi A. Three-dimensional spatial energy-quality map construction for optimal robot placement in multi-robot additive manufacturing. Robot Comput Integr Manuf 2024;88:102735. https://doi.org/10.1016/j.rcim.2024.102735.

[4] Kubalak JR, Wicks AL, Williams CB. Exploring multi-axis material extrusion additive manufacturing for improving mechanical properties of printed parts. Rapid Prototyp J 2019;25:356–62. https://doi.org/10.1108/RPJ-02-2018-0035.

[5] Christ J, Leusink S, Koss H. Multi-axial 3D printing of biopolymer-based concrete composites in construction. Mater Des 2023;235:112410. https://doi.org/10.1016/j.matdes.2023.112410.

[6] Zhang K, Chermprayong P, Xiao F, Tzoumanikas D, Dams B, Kay S, et al. Aerial additive manufacturing with multiple autonomous robots. Nature 2022;609:709–17. https://doi.org/10.1038/s41586-022-04988-4.

[7] Hunt G, Mitzalis F, Alhinai T, Hooper PA, Kovac M. 3D printing with flying robots. Proc - IEEE Int Conf Robot Autom 2014:4493–9. https://doi.org/10.1109/ICRA.2014.6907515.

[8] Nettekoven A, Topcu U. A 3D Printing Hexacopter: Design and Demonstration. 2021 Int Conf Unmanned Aircr Syst ICUAS 2021 2021:1472–7. https://doi.org/10.1109/ICUAS51884.2021.9476759.

[9] Islam R, Nazifa TH, Mohammed SF, Zishan MA, Yusof ZM, Mong SG. Impacts of design deficiencies on maintenance cost of high-rise residential buildings and mitigation measures. J Build Eng 2021;39. https://doi.org/10.1016/j.jobe.2021.102215.

[10] Song X, Pan Y, Chen Y. Development of a low-cost parallel kinematic machine for multidirectional additive manufacturing. J Manuf Sci Eng Trans ASME 2015;137:1–13. https://doi.org/10.1115/1.4028897.

[11] Schuh G, Bergweiler G, Lukas G, Hohenstein S, Schenk J. Feature-based print method for multi-axis material extrusion in additive manufacturing. Procedia CIRP 2020;93:885–90. https://doi.org/10.1016/j.procir.2020.03.024.

[12] Bedarf P, Dutto A, Zanini M, Dillenburger B. Foam 3D printing for construction: A review of applications, materials, and processes. Autom Constr 2021;130:103861. https://doi.org/10.1016/j.autcon.2021.103861.